ORIGINAL ARTICLE

Proton HR-MAS MR spectroscopy of oral squamous cell carcinoma tissues: an ex vivo study to identify malignancy induced metabolic fingerprints

Shatakshi Srivastava · Raja Roy · Vivek Gupta · Ashish Tiwari · Anand N. Srivastava · Abhinav A. Sonkar

Abstract Oral squamous cell carcinoma (SCC) represents more than 90% of all head and neck cancers as reported by Hermans (*Cancer Imaging*, 5(Spec No A), S52–S57, 2005), which draws attention of investigative research for novel predictive metabolic biomarkers to understand the malignancy induced biochemical perturbations occurring at molecular level. In the present work, proton HR-MAS NMR spectroscopic studies have been performed on resected human oral SCC tumor tissues, its neighboring margins and bed tissues ($n = 159$), obtained from 36 patients ($n = 27$ training set; $n = 9$ unknown test set), for the identification of metabolic fingerprints. The proton NMR spectra were then subjected to chemometric unsupervised PCA and supervised OSC-filtered PCA and PLS-DA multivariate analysis. Application of PLS-DA on orthogonally signal corrected training data-set ($n = 120$ tissue specimens; 27 patients) allowed >95% correct classification of malignant tissues from benign samples with >98% specificity and sensitivity. The OSC-PLS-DA model thus constructed was used to predict the class membership of unknown tissue specimens ($n = 39$) obtained from nine patients. These tissue samples were correctly predicted in its respective histological categories with 97.4% diagnostic accuracy. The regression coefficients obtained from OSC-filtered PLS-DA model indicated that malignant tissues had higher levels of glutamate, choline, phosphocholine, lactate, acetate, taurine, glycine, leucine, lysine, isoleucine and alanine, and lower levels of creatine and PUFA, representing altered metabolic processes (lipidogenesis, protein synthesis, and volume regulation) during tumor progression. Thus proton HR-MAS MR spectroscopy could efficiently identify the metabolic perturbations of malignant tumor from non-malignant bed and margins tissue specimens, which may be helpful in understanding the extent of tumor penetration in neighboring tissues.

S. Srivastava · R. Roy (✉)
Centre of Biomedical Magnetic Resonance, Sanjay Gandhi Post-Graduate Institute of Medical Sciences, Rae Bareli Road, Lucknow 226014, Uttar Pradesh, India
e-mail: roy@cbmr.res.in

V. Gupta · A. Tiwari · A. A. Sonkar (✉)
Departments of General Surgery, Chattrapati Shahuji Maharaj Medical University, Lucknow 226001, Uttar Pradesh, India
e-mail: abhinavarunsonkar@gmail.com

A. N. Srivastava
Departments of Pathology, Chattrapati Shahuji Maharaj Medical University, Lucknow, India

Abbreviations

HR-MAS	High resolution magic angle spinning
PCA	Principal component analysis
OSC	Orthogonal signal correction
PLS	Partial least square
NOESY	Nuclear overhauser enhancement spectroscopy
COSY	Correlation spectroscopy
CPMG	Carr Purcell Meiboom Gill sequence
HSQC	Heteronuclear single quantum coherence
SCC	Squamous cell carcinoma

1 Introduction

Oral squamous cell carcinoma (SCC) is sixth most common cancer in the world and constitutes almost 50% of all the cancers diagnosed in males and it represents 90% of all head and neck cancers (Hermans 2005). In USA only oral cancer represents 13% of all cancers thereby translating into 30,000 new cases every year. The annual age-adjusted incidence rates per 100,000 in several European countries vary from 2.0 (UK) to 9.4 (France) while in Asia it ranges from 1.6 (Japan) to 13.5 (India). Studies have shown that the major risk factors for oral SCC are tobacco chewing and excessive alcohol consumption which contribute to degenerative changes described as "pre-cancerous" in oral mucosa (Sinha et al. 2003). Further, the formation of free radicals from environmental contaminants and by other exogenous factors, cause oxidative stress in readily accessible mucosa of oral cavity and then initiate metabolic cascade in cells turning a pre-cancerous lesion into the malignant one (Brandizzi et al. 2008; Hashibe et al. 2007).

The relative 5-year survival rate varies from 81% for localised tumor to approximately 50% for those with regional metastasis to a low 29.5% for distant metastasis (Khandekar et al. 2006). Even aggressive combinations of surgery, radiotherapy and chemotherapy, could not much improve the 5-year survival rates for all stages combined (Boyle and Strong 2001). This poor survival rate is due to development of multiple primary tumors and advanced extent of disease at the time of diagnosis (Donnell et al. 2008). The problem of late presentation of disease could be overcome by the development and use of diagnostic aids that could readily assess the oral lesions. However, numerous radiological investigations like PET, CT and MRI (Cohan et al. 2009; Ng et al. 2006) are available for detection and diagnosis of oral SCC but confirmation comes from histopathology of tumor tissues, still the gold standard technique.

The histopathological analysis cannot explain why certain tumors metastasize while other tumors grow to larger size and remain localised. Therefore, newer methods are required for understanding of intracellular features of post-surgical tumor tissues along with negative margins, including third dimension that is bed of the tumor. This will improve the identification of residual disease after tumor resection and for the better management of disease, as more is the distance of affected marginal tissue from tumor, more the tumor will be aggressive and penetrative. This would also increase the accuracy of diagnosis of the malignant lesions, which when coupled with appropriate therapy, is rewarded with minimal dysfunction and optimal survival.

Numerous studies on genomics and proteomics of oral SCC have been performed in this direction. A recent study demonstrates that Sphingosine kinase-1 (SPHK1) modulates the proliferation, apoptosis and differentiation of keratinocytes through the regulation of ceramide and sphingosine-1-phosphate levels which gets up-regulated in head and neck SCC and may play an important role in tumor progression (Facchinetti et al. 2010). Another genetic study has reported that STK15 is oncogenic for oral SCC and that its nuclear expression is a predictor of clinical behaviour and STK15 copy number is amplified in 12% of oral SCC (Kao et al. 2010). Whereas genomics and proteomics researchers have provided targeted information about alterations at gene and protein level, the HR-MAS NMR spectroscopy can provide simultaneous information about various metabolic derangements which are associated with different disease-specific metabolic processes.

Several reports exist in literature that address the role of ^{1}H HR-MAS NMR Spectroscopy (Cheng et al. 1998; Tugnoli et al. 2004) for the identification of biomarkers in breast cancer (Sitter et al. 2002), colon cancer (Chan et al. 2009), prostate cancer (Cheng et al. 2005; Jordan and Cheng 2007), etc. The technique has successfully demonstrated real insights into the mechanisms of toxicity and pathology at molecular level (Bollard et al. 2000; Duarte et al. 2005; Garrod et al. 2001; Wang et al. 2006). Besides being non-invasive (the same tissue specimen could be used for histopathological examination), the HR-MAS technique greatly enhances spectral resolution and provides relevant biochemical information present in tissues. Earlier studies have shown the ability of high-resolution proton MRS of tissue specimens to differentiate SCC of upper ADT (aero-digestive tract) from uninvolved muscle. The total choline/creatine (Cho/Cr) peak intensity ratio can be used to distinguish tumor from muscle in vitro (Mukherji et al. 1996). A study of SCC of head and neck region has demonstrated the diagnostic potential of ex vivo proton MRS, wherein higher total Cho/Cr ratio along with taurine, glutamic acid and lipids of histopathologically confirmed malignant tissue were observed as compared to normal tissue (Sayed et al. 2002). The higher/lower intensities of metabolic resonances indicate their corresponding concentrations which are directly proportional to the up- or down-regulation of various cellular processes. The present study, therefore, primarily focuses on the identification of metabolic biomarkers for oral SCC using ^{1}H HR-MAS NMR spectroscopy. Secondly, to evaluate the combined contribution of metabolite biomarkers towards diseased state, which make them different from their matched controls, for assessing clinico-pathological status of unknown tissue specimens with the help of multivariate statistical analysis and histopathology of same tissues for confirmation of our findings.

2 Materials and methods

The current study is a prospective ex vivo HR-MAS NMR analysis of malignant (SCC) and non-malignant tissues of oral cavity.

2.1 Chemicals

D_2O (99.96 atom% deuterium-enriched, with 0.03% sodium-3-(trimethylsilyl)-2,2,3,3-d_4-propionate—TSP) was purchased from Sigma–Aldrich Inc. (St. Louis, MO, USA). All other chemicals used were of reagent grade with the highest purity commercially available, unless otherwise mentioned.

2.2 Clinical methods

Tissue specimens ($n = 159$) were obtained from 36 patients (30 males and 6 females) who were enrolled with a written consent to participate in the study that was approved by the ethics committee at Chattrapati Shahuji Maharaj Medical University, Lucknow (formerly King George's Medical University, Lucknow). The mean $\pm$ SD age of 36 patients who were suffering from oral cancer was 50 ± 8.2 years. None of the patients were dehydrated and/or anaemic (mean Hb 11.2 g/dl) at the time of surgery. The staging, histology and grading of all the patients are presented in Table 1 (supplementary material). During surgery, four to six tissue samples weighing 100–200 mg and comprising of tumor and adjacent benign oral mucosa were obtained from each patient with well differentiated SCC. Sampling was purely based on visual screening by the surgeon. Both tumor and peri-tumoral region were sampled up to 4 cm from the edges of the tumor so as to minimize the probability of leaving any cancerous cells, which consisted of adjacent 'margins' of tumor and area underlying tumor or tumor 'bed' left after tumor resection. The margin and bed tissues included histologically proven muscles ($n = 72$), salivary glands ($n = 15$) and inflammatory cells ($n = 4$), present in the surrounding of tumor in oral cavity. All these tissue samples were stored in high-quality plastic vials and snap-frozen in liquid Nitrogen at the time of surgery, to stop all the enzymatic and consequent metabolic activities and were then stored at –80°C till the NMR experiments were performed.

2.3 Tissue samples

The stored tissues were thawed and washed with D_2O prior to NMR analysis, to remove blood and other impurities. The tissues were then dissected carefully and the inner-core (30–40 mg of wet-weight) of the tissues was taken for HR-MAS NMR experiments, to ensure that acquired spectra exhibits resonances from tumor only. Typically, the sample was packed into a 4 mm ZrO_2 rotor of 50 μl capacity; a volume of 20 μl of D_2O having 0.03% TSP was used as a chemical shift reference. The sample-rotor-setup was then transferred into the HR-MAS NMR probe.

2.4 Magnetic resonance spectroscopy

The proton HR-MAS NMR spectra were recorded on a Bruker Avance 400 MHz spectrometer equipped with a 4 mm HR-MAS ^1H-^{13}C dual probehead with magic-angle gradient, operating at a proton frequency of 400.13 MHz. In all NMR experiments, the samples were spun at 4.0 kHz in order to eliminate the signals arising due to rotation sidebands. Proton NMR spectra with water suppression were acquired using one-dimensional NOESY pulse-sequence with the following experimental parameters: mixing time τ_m of 100 ms, total relaxation time of 3.99 s, spectral width of 8,250.8 Hz, 128 transients with a total recording time of 9 min. Additionally, one-dimensional CPMG (Carr-Purcell-Meiboom-Gill; Wang et al. 2003) experiment with water suppression was recorded with an echo-time of 160 ms for each tissue sample. The sample temperature was maintained at 283 K using cooled nitrogen gas during the acquisition of the spectra.

The two-dimensional COSY experiment with water suppression was carried out on a few tissue specimens with the following experimental parameters: A spectral width of 4,807.69 Hz, 2.2 s relaxation delay, 128 transients, and 256 time increments (t1) were acquired corresponding to a total acquisition time of 7 h. The raw data was zero-filled up to 512 words (w) with sine-bell window function prior to double Fourier transformation. Two-dimensional gradient ^1H-^{13}C HSQC experiment was performed using adiabatic pulses on few tissue specimens with water suppression. For this experiment, a total relaxation delay of 1.6 s was used; 128 transients were averaged for each 128 t1 corresponding to a total acquisition time of 8 h. The raw data was zero-filled up to 1,024 w and weighted with 90° shifted square-sine-bell window function prior to double Fourier transformation. One-dimensional CPMG spectra with presaturation were acquired for few tumor tissues for observing time dependent sample decay, if any. However, no significant differences were observed in the spectral metabolite pattern even after subjecting the tissue specimens for approximately one hour long NMR measurements (supplementary material), which is supported by earlier HR-MAS studies on cancer tissue specimens (Rocha et al. 2010; Wilson et al. 2009). Furthermore, the tissue specimens showing only lipid resonances (comprising of margins and bed) were re-dissected from the main sample and again subjected to NMR measurements, so as to eliminate the probability of analyzing any wrong section of tissue.

2.5 Histopathology

After spectroscopic analysis, the tissue samples were initially fixed in 10% formalin, and were further embedded using paraffin. Sections of 5 mm at 100 μm intervals were taken to include the whole tissue specimen and were stained using haematoxylin and eosin. Sections were assessed whether or not a tissue specimen proved to be malignant. Overall, 78 tissue specimens including tumor, margins and bed obtained, after surgery, were identified to have well-differentiated SCC. Figure 1 depicts the spectra obtained from non-malignant and malignant tissues along with their respective histopathology.

2.6 Statistical analysis

The external calibration of the data was performed by dividing ∼75% of the patients as training set and the remaining ∼25% as test set. In the present study, out of 36 patients ($n = 159$ tissue specimens), 27 patients were randomly selected from Fisher and Yates table (Fisher and Yates 1957) as training set for OSC-filtered PLS-DA model generation and the rest 9 patients (39 specimens) were

predicted on the basis of that model. The training set comprised of 120 tissue specimens with 52 tissues ($n = 3$ bed; $n = 15$ margin; $n = 34$ tumor tissues) having malignant histology while rest 68 ($n = 32$ bed; $n = 36$ marginal tissues) were benign in nature. The nine patients, comprising the test set, were not included while construction of the model as the authors were kept blinded from the class-membership of corresponding tissue specimens ($n = 39$) till the prediction of their respective pathological status and were then compared with their corresponding histopathology reports.

2.7 NMR data reduction and pattern recognition

Both NOESY and CPMG spectra were acquired from tissue samples but only CPMG spectra were subjected for further multivariate analysis as a clear profile of small metabolite biomarkers is obtained due to suppressed resonances from high molecular weight components. Since variations in small metabolite concentrations represent corresponding alterations in intracellular processes, region from 1.80–4.25 ppm was considered so that short T_2 components could be maximally avoided for both OSC
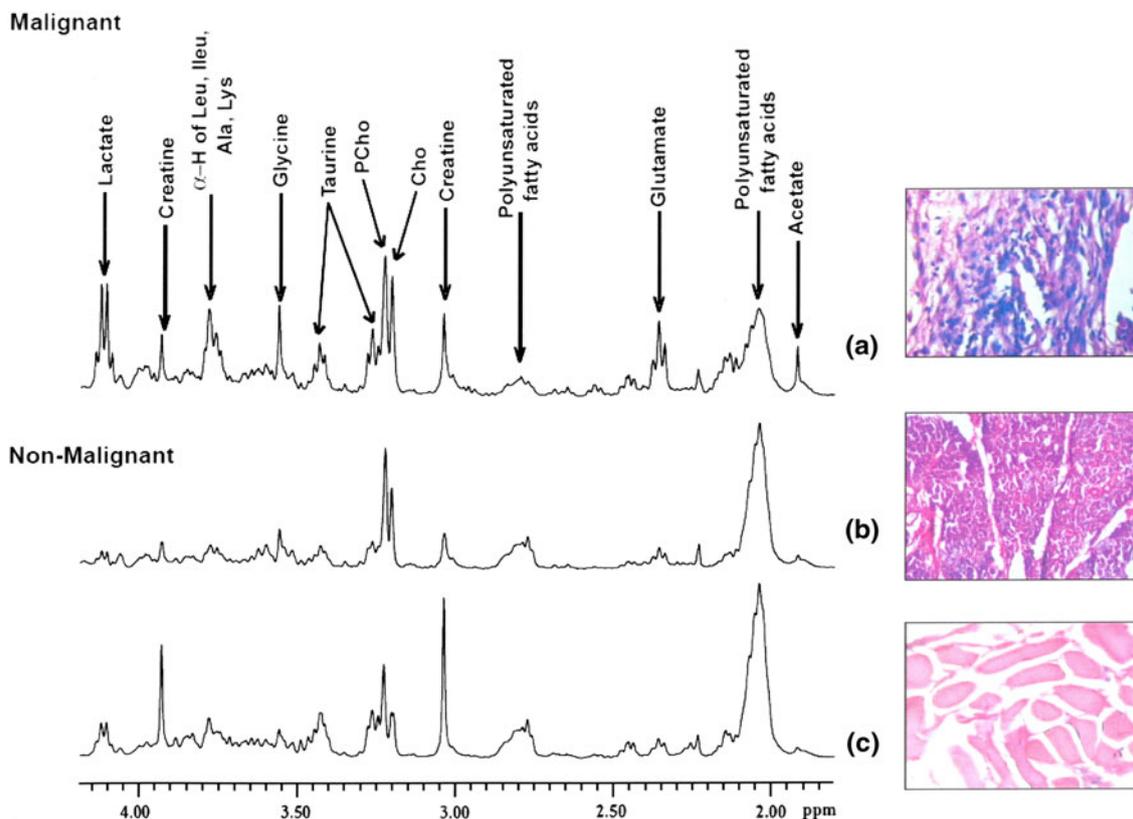
Fig. 1 High resolution magic angle spinning ^{1}H MR spectrum obtained from: **a** malignant oral SCC tissue, **b** its non-malignant adjacent marginal salivary gland tissue, and **c** neighboring non-malignant muscle tissue (*bed*) and the corresponding histopathological analysis of the same tissues after its spectroscopic analysis. Cellular metabolites mentioned in the text are labeled in the spectrum

filtered PCA and PLS-DA. The spectral complexity of CPMG spectra were reduced by binning the region of 1.80–4.25 ppm to 245 continuous integral segments of equal width of 0.01 ppm by using AMIX software (version 3.7.10, Bruker BioSpin, Switzerland). The data obtained was mean centered, scaled to unit variance and then normalized by dividing each integral segment by total area of the spectrum in order to compensate for the differences in overall metabolite concentration between individual tissue specimens. This resulted in a data matrix, which was then exported to 'The Unscrambler X' Software package (Version 10.0.1, Camo ASA, Norway) for multivariate analysis. PCA was performed on data matrix for the detection of any separation trends and then OSC filtered PCA and PLS-DA modeling was done, in which the histopathology report of each tissue specimen was used as the one-component Y-matrix. OSC-PCA and PLS modeling was performed by applying OSC filter to the data matrix, prior to PLS regression (Brindle et al. 2002; Gavaghan et al. 2002). In each analysis, sevenfold cross validation step was performed to avoid over-fitting of the model.

3 Results

3.1 NMR spectral assignments

The HR-MAS proton spectra provided well-resolved resonances for most of the commonly observed metabolites that were assigned on the basis of previously reported values available in the literature (Bisbal et al. 2004; Cheng et al. 1997b, 1998; Tugnoli et al. 2004). The two-dimensional COSY and HSQC experiments were performed on few tissue samples to confirm the assignments of resonance in our spectra (supplementary material, Table 2). The singlet signal at 3.03 ppm, arising due to the methyl group of creatine, was used as an internal chemical shift reference. Apart from prominently observed lipid resonances, the small metabolites identified include leucine (Leu), isoleucine (Ileu), valine (Val), lysine (Lys), alanine (Ala), lactate (Lac), threonine, acetate (Ace), glutamate (Glu), glutamine, methionine, aspartic acid, citrate, asparagine, tyrosine, phenylalanine, ethanolamine, choline (Cho), phosphocholine (PCho), glycerophosphocholine, *myo*-inositol, taurine, α- and β-glucose, triglyceride, glycine (Gly) and creatine (Cr).

3.2 Statistical interpretation

The present work has been undertaken with an aim of correlating spectral metabolite profiles with clinico-pathological status of patients. Since pathological processes are likely to induce simultaneous changes in an ensemble of

metabolites, alteration in the level of a single metabolite may not provide the required insight regarding the biochemical processes occurring at cellular level. Hence, prior to investigating aforesaid correlations, the ensemble of CPMG spectra was subjected to PCA to reduce the spectral complexity. Score-plot of the first (PC1) and second (PC2) principal components and its corresponding loading plot has been shown in Fig. 2a.

The input variables required for this purpose were originally obtained from the spectral/bucket loading-profile as shown in Fig. 2b. Variations occurring in the metabolic profile of malignant and non-malignant tissue specimens could be seen based on clustering of spectra in the PC score-plot. Since PCA scores were suggestive of group separation, orthogonal signal correction was applied for enhancing the predictive power of the model which resulted in better group separation (Beckwith-Hall et al. 2002; Brindle et al. 2002). In addition, Fig. 2b highlights the altered levels of those metabolites which were responsible for such clustering; in fact, variables contributing to similar information have grouped themselves together in a cluster. Figure 2c and d show OSC filtered PC1 versus PC2 (Brindle et al. 2002; Gavaghan et al. 2002) scores of PCA, and PLS-regression score plots of the tissue specimens are presented in Fig. 2e and f. The regression coefficients (Fig. 2f) of OSC-PLS DA indicated the regions of the spectra that contributed for the clustering of each group. The malignant clustering occurs due to increased levels (Fig. 2c and f) of acetate (1.90 ppm), glutamate (2.35 ppm), taurine (3.23 ppm), choline (3.20 ppm), phosphocholine (3.21 ppm), glycine (3.56 ppm), lactate (4.12 ppm) and α-H of Leu, Ileu, Val, Lys, Ala (3.76–3.79 ppm).

The information gathered from clustering in PCA had suggested that malignancy induces metabolic perturbations at cellular levels, and therefore, a supervised OSC-filterd PLS-DA model was developed to achieve improved separation between the groups defined a priori in a way to minimize misclassification error rates arising due to gender, diet, age and medication (Beckwith-Hall et al. 2002). Hence, the model was prepared on training set as shown in Fig. 2e. In the training model, >98% sensitivity and specificity were achieved. In order to ensure sufficient robustness, the training set was cross-validated by random seven-fold cross-validation method. The training model thus prepared was used to predict the class membership of the unknown tissue samples of test set ($n = 39$). The Y-predicted OSC-PLS graph (Fig. 3) assigned samples to either class 0 (malignant) or class 1 (benign) using a priori cut-off of 0.5 and showed the ability of ^{1}H HR-MAS NMR to predict class membership of unknown samples with 97.4% diagnostic accuracy (100% sensitivity; 92.3% specificity).
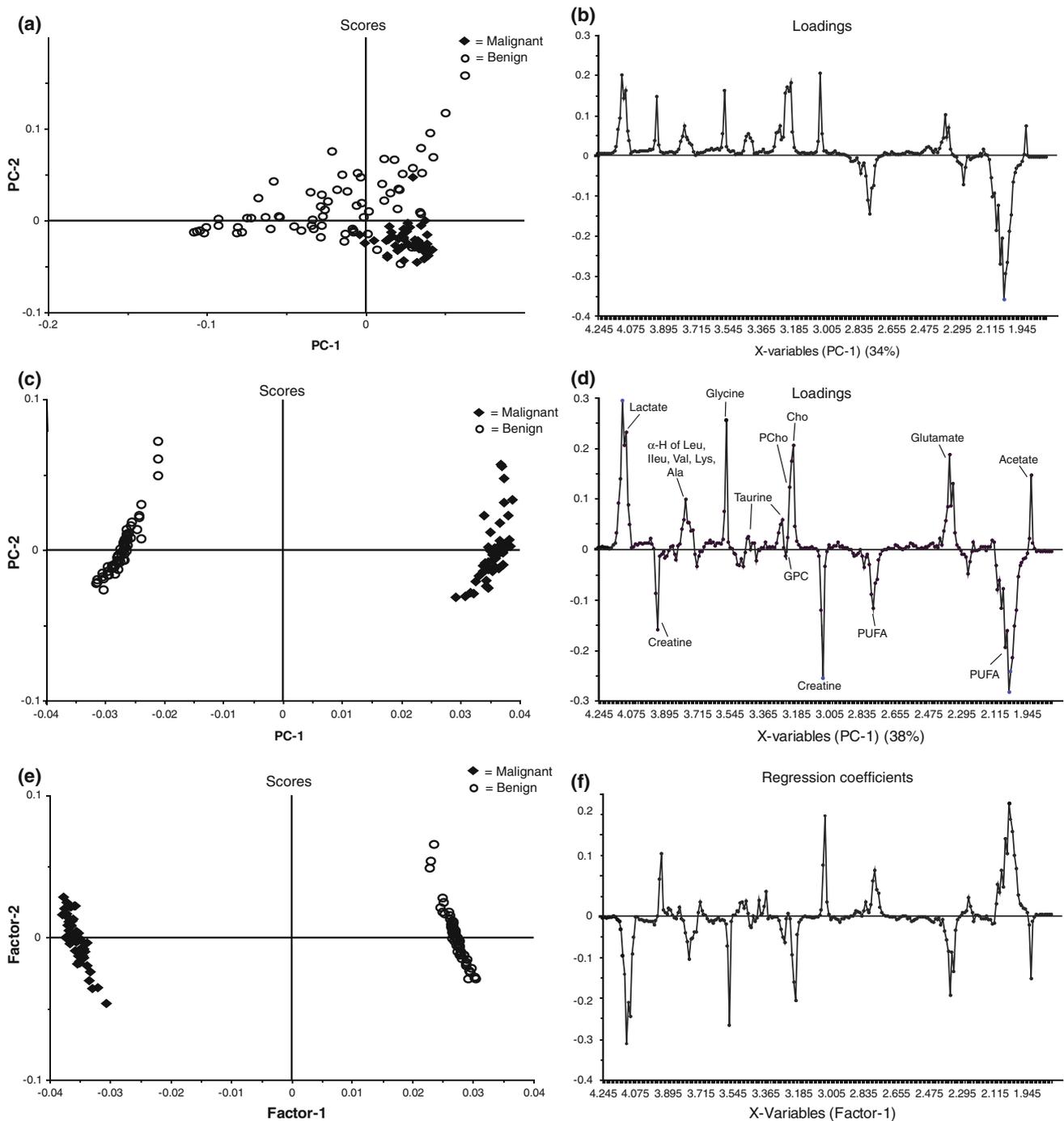
Fig. 2 **a** PC1 versus PC2 score plot derived from ^{1}H HR-MAS NMR spectra of tissues obtained from 36 patients. The samples are marked according to their malignant and benign categories as marked in the legend. **b** The corresponding loading plot. **c** PC score plot after application of orthogonal signal correction on 120 tissue samples from 27 patients. **d** The corresponding longitudinal loading plot where positive values indicates higher concentrations of metabolites in oral SCC and vice versa for negative values. **e** The PLS-DA score plot after application of the OSC to remove uncorrelated variance components. **f** The regression coefficients for PLS-DA model using OSC-transformed data

4 Discussion

The neoplastic alterations in Kreb's cycle and consequent alterations in normal cellular processes eventually result in malignancy. Humans continue to succumb to cancer, as manifestation of first malignancy increases the risk of recurrence in nearby cells. The initial lesion announces a general susceptibility to adjacent tissues and, therefore,
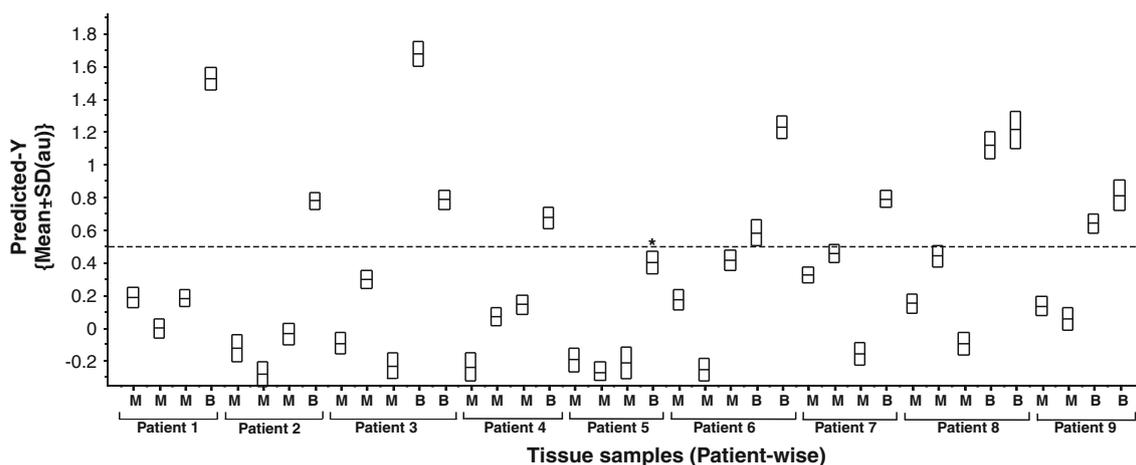
Fig. 3 Prediction of oral SCC status using OSC-filtered PLS-DA model which was prepared on 120 tissue samples obtained from 27 patients (training set). This model was then used to predict the tissue pathology status of 39 tissue specimens obtained from 9 patients (test set). The predictions are made on the basis of a priori cut-off value of 0.5 for class membership, using Y-predicted box-plots (class 0 for oral SCC and class 1 for benign group). The predicted mean values along with standard deviation are depicted, where $B =$ benign and $M =$ malignant tissue specimens as per histological reports. (* = misclassification)

analysis of margins and bed of tumor may define the extent of tumor dispersion, thereby aiding in improved prognosis. If the affected margins are not resected properly, they may result in recurrence and therapeutic failure, making the situation worse. In this regard, several attempts have been made to improve the diagnosis of oral SCC and to establish predictive factors related to tumor biology (Mashberg and Samit 1995). This study aims to define the potential of HR-MAS NMR spectroscopy for a better post-surgical management of oral SCC patients by defining the malignancy status of neighbouring margins and bed of the tumor. The two important findings of this study are: (i) increased levels of Ace, Glu, Lac, Cho, PCho, Gly, Tau, Leu, Ileu, Val, Lys, Ala and decreased levels of polyunsaturated fatty acids and creatine in malignant tumors as obtained from the loading plots of OSC-PLS DA analysis and (ii) the metabolic alterations of malignant tumors could be distinctly identified from the non-malignant tissues by ^{1}H HR-MAS NMR spectroscopy, which may acknowledge the presence of residual disease in neighboring tissues after resection of the tumor.

The interpretation of PCA model without OSC (Fig. 2a) to establish the metabolic differences between the two groups was delimited by the influence of physiological variations (Beckwith-Hall et al. 2002). The corresponding loading plot (Fig. 2b) represented the regions of NMR spectrum that most strongly influence the separation between oral SCC and control tissue samples. The partial overlapping of two groups was suggestive of group separation which indicated that removal of confounding variations from the data set would focus the interpretation of model only on disease-related variations. After application of OSC, the well-separated groups of oral SCC and control

samples in PCA and PLS-DA were obtained (Fig. 2c and d). The positive values in regression plot indicated higher concentration of metabolites in benign tissues and a negative value indicates relatively higher concentration with respect to oral SCC tissue specimens. The regression coefficients indicated that acetate (1.90 ppm), glutamate (2.35 ppm), taurine (3.23 ppm), choline (3.20 ppm), phosphocholine (3.21 ppm), glycine (3.56 ppm), lactate (4.12 ppm) and α-H of Leu, Ileu, Val, Lys, Ala (3.76–3.79 ppm) were present in higher concentration in malignant samples as compared to the controls while PUFA and creatine were present in relatively lower concentration.

As a rule of thumb, larger samples more accurately represent the characteristics of the population from which they are derived (Green 1991; Voorhis and Morgan 2007). Thus, larger sample size increase power of prediction, decrease estimation error and thus improve the robustness and precision of the model. Therefore, patients were divided into 75:25 ratio rather than equally dividing them. The prediction of class-membership of unknown tissue specimens of test data set with 97.4% diagnostic accuracy by PLS-DA model indicated the robustness of model and established that separation observed between two groups in OSC-PLS-DA score plot was due to significant cancer related variations in the spectral profile of tissues (Fig. 3).

In our study, there is an observed decrease in polyunsaturated fatty acids (PUFA) concentration in cancer cells which may be due to the modifications in lipid composition under malignant conditions. These modifications include decrease in PUFA which consequently cause alterations in membrane bilayer fluidity and enzymatic activities at the level of mitochondrial and microsomal membranes, which

has been proved by an earlier biochemical study on rapidly growing hepatoma cells (Crain et al. 1983; Morton et al. 1977). Also an earlier ex vivo MRS study on the prediction of treatment response in head- and neck cancer has shown significant differences in spectral intensity ratios of choline-containing metabolites (3.2/3.0 ppm) and mobile lipids at 1.3/0.9 ppm (Bezabeh et al. 2005) which confirms our finding.

Malignant cells exhibit uncontrolled rates of cell division and this process requires lipids, amino-acids and other small metabolites to support key biosynthetic pathways. Variations in these metabolite concentrations reflect changes in metabolism arising from biologic condition of disease. Thereby, in this study emphasis had been laid upon small metabolites which provide a true picture of cell proliferation and the altered cellular processes. The higher levels of Lac, PCho, Cho, amino acids and lower levels of PUFA and Cr were found only in typical SCC as compared to non-malignant cases; this is in concordance with the metabolic alterations occurring in malignant cells during cell-proliferation, as it requires nutrients, energy and higher biosynthetic activity to duplicate all macromolecular components during each passage through cell-cycle while maintaining the cancer cell homeostasis. Therefore, cellular processes occurring in malignant cells are quite different from those of non-proliferating cells. The higher lactate levels have been observed in our study (Fig. 1) as Otto Warburg (Warburg 1956) reported that metabolic activities of malignant cells show high glycolytic rates and reduced mitochondrial oxidation, which favors the cell-survival in hypoxic micro-environment of tumor; also, glucose to lactate conversion protects malignant cells from oxidative stress (due to reactive oxygen species) resulting in high lactate accumulation as a pronounced consequence (McFate et al. 2008). Apart from lactate, higher levels of alanine are also attributed to the hypoxic conditions of malignant tumors (Griffin and Shockcor 2004).

The rapid proliferation of cancer cells also affects their energy requirement which are fulfilled by high-energy creatine phosphate, which is formed from creatine by the mediation of enzyme creatine kinase (Podo 1999). The formation of high energy phosphates result in creatine deficit in the cells which has been reinstated by our findings. An in vitro proton MRS study of extra-cranial head and neck SCC had shown significant elevation in the Cho/Cr ratio (Mukherji et al. 1997). In the present investigation using HR-MAS, broad resonances due to choline-containing compounds are well-resolved in the CPMG spectrum, providing precise information about the metabolic perturbations occurring in cancer cells. Choline (3.20 ppm) is known to play a key role in phospholipid metabolism of cell membranes, and represent active cell proliferation in the form of increased membrane phospholipid turnover.

The phosphorylation of choline results in PCho, which is followed by a cascade of biochemical reactions to form phosphatidylcholine. Phosphatidylcholine is a major phospholipid component of eukaryotic cells which participates in lipid metabolism, signal transduction mechanisms and in membrane structure (Podo 1999). Thus, higher Cho and PCho contents are well-known markers of increased cell proliferation in the cancer cells. Apart from Cho and PCho, higher level of acetate was also observed which may be attributed to the increased lipid biosynthesis and altogether these three metabolites reflect highly active proliferation of tumor cells.

The increased glutamate levels in SCC tissues reconfirm a recent study on tumor growth which has shown that glutamate stimulates proliferation and migration of tumor cells (Rzeski et al. 2001) and thus facilitates the tumor progression. Glycine is an amino acid which is reportedly an essential precursor for de novo purine formation (an integral part of nucleic acids) as shown by an earlier study on breast tumor cell lines (Griffin and Shockcor 2004). Hence, its higher concentration in malignant tumors is a marker for enhanced nucleotide synthesis.

The unique feature of cancer as a disease is the capacity of the disease itself to use amino acids for its own metabolism and proliferative activities. The cancer cells utilize glutamine, alanine and glycine along with other branched chain amino acids for its protein biosynthesis (Baracos and Mackenzie 2006; Norton et al. 1981), which increases manifold in malignant tissues for their proper progression and proliferation (Tessem et al. 2008). This fact is reflected by the significant increase in the relative intensities of these metabolites in NMR spectra of the malignant tissues. Not only enhanced protein synthesis, lipidogenesis and nucleic acid formation contribute in unhindered cancer proliferation but volume regulation and osmoregulation also play an equally important role in it. Taurine acts as an osmolyte (Griffin and Shockcor 2004) and its higher concentration probably helps in controlling hypoxia induced cell swelling (Shen et al. 2001; Srivastava et al. 2010), thereby maintain the cell volume. Taurine also acts as a free-radical scavenger for reducing the oxidative stress of the cells and their unhindered proliferation (Rosado et al. 2007). Earlier studies on various cancers have shown that taurine concentration is higher in various tumors. All these metabolites act as biomarkers for the suppression or aggravation of different cellular processes occurring in cancer cells and therefore, play an important role in distinguishing normal tissues from the malignant ones.

In this study, the malignant tissue samples comprising of histologically-proven tumor, bed ($n = 3$) and neighboring margins ($n = 15$), were present in the same group in OSC-filtered PCA and PLS-DA which highlighted that adjacent

margins and bed should be given special attention to aid in better diagnosis and treatment, as primary lesions develop a field of cancerisation where various genetic aberrations occur in mucosa and play a crucial role in tumorigenesis (van Houten et al. 2004). Earlier genetic studies have shown that in 52% of patients with histologically-negative margins have same p53 mutations as those present in tumor (Brennan et al. 1995) and second primary tumors develop more frequently when p53 mutations are present in tumor-distant mucosa (Waridel et al. 1997). Since numerous studies have reported that tumor-positive surgical margins are an important source of treatment failure and recurrence (Partridge et al. 2000), therefore, successful removal of such margins and bed tissues from the disease site minimizes the probability of recurrence in patients resulting in better survival rate.

A current limitation of our study is that it cannot differentiate among different tissue types like salivary glands and muscles but can be used as a reliable analytical tool for classifying malignant tissues from non-malignant ones, in conjunction with histopathology. Because histopathological assessment is so important for staging, prognosis, and therapeutic intervention in most kinds of tumors, the addition of HR-MAS NMR spectroscopic analysis may have far-reaching implications. The above mentioned limitation of this study may be attributed to the smaller sample size, therefore, large population studies are required to ensure the role of these biomarkers in cancer cells and the study can be further extended to understand the aggressiveness of the tumor including metastasis.

Since tissue extraction methods may modify original cellular metabolic composition to an unknown extent, particularly the proportion of acetate and choline derivatives (Cheng et al. 1997a), these procedures may cause erroneous correlation between diseased state and MRS results. Furthermore, tumor heterogeneity limits the utility of extraction processes (Cheng et al. 2000) while in in vivo studies, peaks being broad in nature may mask the signals arising from neighboring protons. HR-MAS spectroscopy has been employed to overcome such modifications in metabolic profile of tissue samples, and the spectral resolution is quite comparable to that of solution state NMR. The overall representation of metabolic alterations in this prospective ^{1}H HR-MAS NMR study goes hand-in-hand with the tumor biology, which is explained by the results of multivariate statistical analyses. In other words, the metabolic fingerprints are easily identifiable for oral tissues having SCC.

The results obtained in the present study may contribute to the evaluation of tumor biochemistry and its point to point correlation with histopathology suggests its clinical relevance and it may further augment our understanding of cancer cell metabolism at the level of metabolic activity.

Therefore, it could be anticipated that such classification models based on metabolite catalogue of tissue biopsies obtained from larger population may contribute to the establishment of ^{1}H HR-MAS NMR as a diagnostic procedure for oral SCC. Thus, simultaneous analysis of metabolic changes with ^{1}H HR-MAS NMR, in conjunction with subsequent histopathology of the same tumor specimen will ultimately improve accuracy in diagnosing, characterizing and evaluating tumor progression.

Since, the spectral measurements were directly conducted with intact tissue specimens, therefore, results obtained are closely related to the in vivo status of tumors. Ex vivo and in vivo NMR spectral peak observations in pathological states can support the reliability of clinical applications by providing more precise information about the biochemical status of the disease. Earlier studies on brain tumors reinforce this fact by determining the relationship between in vivo and ex vivo biochemical characterization of brain tumors by using MR spectroscopy (Tzika et al. 2002; Wilson et al. 2009). Further extensions of the present study may involve in vivo multi-voxel magnetic resonance spectroscopic imaging of oral SCC tumor and its correlation to the metabolic biomarkers obtained from ex vivo NMR studies for identifying the aggressiveness of the tumor. Such studies will contribute to the better management of the patients suffering from oral SCC.

5 Conclusion

In summary, the malignant tissues possess a distinct signature of altered cellular processes which makes it quite distinguishable from non-malignant tissues. The present investigation involving oral SCC has highlighted the efficacy of ^{1}H HR-MAS NMR spectroscopy in identifying the altered metabolic processes in tumor tissues. The bed, margins and tumor-core were individually analyzed to assess the presence of tumor and its penetration in bed and underlying tissues, involving their metabolite catalog. The positive histological confirmation of malignancy for neighboring margins and bed tissues emphasizes on the fact that such measurements might revolutionize the assessment of residual disease after the resection of tumor. This study offers an insight of cancerous processes occurring in tumor tissues.

Another advantage with this technique is that it maintains the actual status of tissues as there are no extraction or derivatization processes involved like other analytical methods including GC–MS and HPLC. This study shows that HR-MAS may resolve the dilemma on extent of tumor penetration in clinical scenario in conjunction with histopathology.

References

Baracos, V. E., & Mackenzie, M. L. (2006). Investigations of branched-chain amino acids and their metabolites in animal models of cancer. *Journal of Nutrition, 136*(1 Suppl), 237S–242S.

Beckwith-Hall, B. M., Brindle, J. T., Barton, R. H., et al. (2002). Application of orthogonal signal correction to minimise the effects of physical and biological variation in high resolution 1H NMR spectra of biofluids. *Analyst, 127*(10), 1283–1288.

Bezabeh, T., Odlum, O., Nason, R., et al. (2005). Prediction of treatment response in head and neck cancer by magnetic resonance spectroscopy. *American Journal of Neuroradiology, 26*(2), 2108–2113.

Bisbal, M. C. M., Bonmati, L., Piquer, J., et al. (2004). 1H and 13C HRMAS spectroscopy of intact biopsy samples ex vivo and in vivo 1H MRS study of human high grade gliomas. *NMR in Biomedicine, 17*(2), 191–205.

Bollard, M. E., Garrod, S., Holmes, E., et al. (2000). High-resolution (1)H and (1)H-(13)C magic angle spinning NMR spectroscopy of rat liver. *Magnetic Resonance in Medicine, 44*(2), 201–207.

Boyle, J. O., & Strong, E. W. (2001). *Oral cavity cancer*. London: BC Decker Inc.

Brandizzi, D., Gandolfo, M., Velazco, M. L., Cabrini, R. L., & Lanfranchi, H. E. (2008). Clinical features and evolution of oral cancer: A study of 274 cases in Buenos Aires, Argentina. *Medicinia Oral, Patologia Oral y Cirugia Bucal, 13*(9), E544–E548.

Brennan, J. A., Mao, L., Hruban, R. H., et al. (1995). Molecular assessment of histopathological staging in squamous-cell carcinoma of the head and neck. *New England Journal of Medicine, 332*(7), 429–435.

Brindle, J. T., Antti, H., Holmes, E., et al. (2002). Rapid and noninvasive diagnosis of the presence and severity of coronary heart disease using 1H-NMR-based metabonomics. *Nature Medicine, 8*(12), 1439–1444.

Chan, E. C., Koh, P. K., Mal, M., et al. (2009). Metabolic profiling of human colorectal cancer using high-resolution magic angle spinning nuclear magnetic resonance (HR-MAS NMR) spectroscopy and gas chromatography mass spectrometry (GC/MS). *Journal of Proteome Research, 8*(1), 352–361.

Cheng, L. L., Ma, M. J., Becerra, L., et al. (1997a). Quantitative neuropathology by high resolution magic angle spinning proton magnetic resonance spectroscopy. *Proceedings of the National Academy of Sciences of the United States of America, 94*(12), 6408–6413.

Cheng, L. L., Ma, M. J., Becerra, L., et al. (1997b). Quantitative neuropathy by high resolution magic angle spinning proton mgnetic resonance spectroscopy. *Proceedings of the National Academy of Sciences of the United States of America, 94,* 6408–6413.

Cheng, L. L., Chang, W. I., Louis, D. N., & Gonzalez, R. G. (1998). Correlation of High-Resolution Magic Angle Spinning Proton Magnetic Resonance Spectroscopy with histopathology of Intact Human Brain Tumor Specimens. *Cancer Research, 58,* 1825–1832.

Cheng, L. L., Anthony, D. C., Comite, A. R., et al. (2000). Quantification of microheterogeneity in glioblastoma multiforme with ex vivo high resolution magic-angle spinning (HRMAS) proton magnetic resonance spectroscopy. *Neuro-Oncology, 2*(2), 87–95.

Cheng, L. L., Burns, M. A., Taylor, J. L., et al. (2005). Metabolic characterization of human prostate cancer with tissue magnetic resonance spectroscopy. *Cancer Research, 65*(8), 3030–3034.

Cohan, D. M., Popat, S., Kaplan, S. E., et al. (2009). Oropharyngeal cancer: current understanding and management. *Current Opinion in Otolaryngology & Head and Neck Surgery, 17*(2), 88–94.

Crain, R. C., Clark, R. W., & Harvey, B. E. (1983). Role of lipid transfer proteins in the abnormal lipid content of Morris hepatoma mitochondria and microsomes. *Cancer Research, 43*(7), 3197–3202.

Donnell, A., Jin, S., & Zavras, A. I. (2008). Delay in diagnosis of oral cancer. *Journal of Stomatological Investigation, 2*(1), 15–26.

Duarte, I. F., Stanley, E. G., Holmes, E., et al. (2005). Metabolic assessment of human liver transplants from biopsy samples at the donor and recipient stages using high-resolution magic angle spinning 1H NMR spectroscopy. *Analytical Chemistry, 77*(17), 5570–5578.

Facchinetti, M. M., Gandini, N. A., Fermento, M. E., et al. (2010). The expression of sphingosine kinase-1 in head and neck carcinoma. *Cells, Tissues, Organs, 192*(5), 314–324.

Fisher, R. A., & Yates, F. (1957). *In statistical tables for biological, agricultural and medical research*. London: Oliver and Boyd.

Garrod, S., Humpher, E., Connor, S. C., et al. (2001). High-resolution 1H NMR and magic angle spinning NMR spectroscopic investigation of the biochemical effects of 2-bromoethanamine in intact renal and hepatic tissue. *Magnetic Resonance in Medicine, 45*(5), 781–790.

Gavaghan, C. L., Wilson, I. D., & Nicholson, J. K. (2002). Physiological variation in metabolic phenotyping and functional genomic studies: Use of orthogonal signal correction and PLS-DA. *FEBS Letters, 530*(1–3), 191–196.

Green, S. B. (1991). How many subjects does it take to do a regression analysis. *Multivariate Behavioral Research, 26*(3), 499–510.

Griffin, J. L., & Shockcor, J. P. (2004). Metabolic profiles of cancer cells. *Nature Reviews Cancer, 4*(7), 551–561.

Hashibe, M., Brennan, P., Benhamou, S., et al. (2007). Alcohol drinking in never users of tobacco, cigarette, smoking in non-drinkers and the risk of head and neck cancer: pooled analysis in the International Head and Neck Cancer. *Journal of the National Cancer Institiute, 99,* 777–789.

Hermans, R. (2005). Oropharyngeal cancer. *Cancer Imaging, 5*(Spec No A), S52–S57.

Jordan, K. W., & Cheng, L. L. (2007). NMR-based metabolomics approach to target biomarkers for human prostate cancer. *Expert Review of Proteomics, 4*(3), 389–400.

Kao, S. Y., Chen, Y. P., Tu, H. F., et al. (2010). Nuclear STK15 expression is associated with aggressive behaviour of oral carcinoma cells in vivo and in vitro. *Journal of Pathology, 222*(1), 99–109.

Khandekar, S. P., Bagdey, P. S., & Tiwari, R. R. (2006). Oral cancer and some epidemiological factors: A hospital based study. *Indian Journal of Community Medicine, 31*(3), 157–159.

Mashberg, A., & Samit, A. (1995). Early diagnosis of asymptomatic oral and oropharyngeal squamous cancers. *CA: A Cancer Journal for Clinicians, 45,* 328–351.

McFate, T., Mohyeldin, A., Lu, H., et al. (2008). Pyruvate dehydrogenase complex activity controls metabolic and malignant phenotype in cancer cells. *Journal of Biological Chemistry, 283*(33), 22700–22708.

Morton, R., Waite, M., Hartz, J. W., Cunningham, C., & Morris, H. P. (1977). The composition and metabolism of microsomal and mitochondrial membrane lipids in the Morris 7777 hepatoma. *Advances in Experimental Medicine and Biology, 92,* 381–403.

Mukherji, S. K., Schiro, S., Castillo, M., et al. (1996). Proton MR spectroscopy of squamous cell carcinoma of the upper aerodigestive tract: In vitro characteristics. *American Journal of Neuroradiology, 17,* 1485–1490.

Mukherji, S. K., Schiro, S., Castillo, M., et al. (1997). Proton MR spectroscopy of squamous cell carcinoma of the extracranial head and neck: in vitro and in vivo studies. *American Journal of Neuroradiology, 18,* 1057–1072.

Ng, S. H., Yen, T. C., Chang, J. T., et al. (2006). Prospective study of [18F] fluorodeoxyglucose positron emission tomography and computed tomography and magnetic resonance imaging in oral cavity squamous cell carcinoma with palpably negative neck. *Journal of Clinical Oncology, 24*(27), 4371–4376.

Norton, J. A., Shamberger, R., Stein, T. P., Milne, G. W., & Brennan, M. F. (1981). The influence of tumor-bearing on protein metabolism in the rat. *Journal of Surgical Research, 30*(5), 456–462.

Partridge, M., Li, S. R., Pateromichelakis, S., et al. (2000). Detection of minimal residual cancer to investigate why oral tumors recur despite seemingly adequate treatment. *Clinical Cancer Research, 6*(7), 2718–2725.

Podo, F. (1999). Tumor phospholipid metabolism. *NMR in Biomedicine, 12,* 413–439.

Rocha, C. M., Barros, A. S., Gil, A. M., et al. (2010). Metabolic profiling of human lung cancer tissue by 1H high resolution magic angle spinning (HRMAS) NMR spectroscopy. *Journal of Proteome Research, 9*(1), 319–332.

Rosado, J. O., Salvado, M., & Bonatto, D. (2007). Importance of the trans-sulfuration pathway in cancer prevention and promotion. *Molecular and Cellular Biochemistry, 301*(1–2), 1–12.

Rzeski, W., Turski, L., & Ikonomidou, C. (2001). Glutamate antagonists limit tumor growth. *Proceedings of the National Academy of Sciences of the United States of America, 98*(11), 6372–6377.

Sayed, S. E., Bezabeh, T., Odlum, O., et al. (2002). An ex vivo study exploring the diagnostic potential of 1H magnetic resonance spectroscopy in squamous cell carcinoma of the head and neck region. *MRS of Head and Neck Tumors, 24,* 766–772.

Shen, M. R., Chou, C. Y., & Ellory, J. C. (2001). Swelling-activated taurine and K + transport in human cervical cancer cells: association with cell cycle progression. *Pflugers Archiv: European Journal of Physiology, 441*(6), 787–795.

Sinha, R., Anderson, D. E., McDonald, S. S., & Greenwald, P. (2003). Cancer risk and diet in India. *Journal of Postgraduate Medicine, 49,* 222–228.

Sitter, B., Sonnewald, U., Spraul, M., Fjosne, H. E., & Gribbestad, I. S. (2002). High-resolution magic angle spinning MRS of breast cancer tissue. *NMR in Biomedicine, 15*(5), 327–337.

Srivastava, S., Roy, R., Singh, S., et al. (2010). Taurine—a possible fingerprint biomarker in non-muscle invasive bladder cancer: A pilot study by 1H NMR spectroscopy. *Cancer Biomarkers: Section A of Disease Markers, 6*(1), 11–20.

Tessem, M. B., Swanson, M. G., Keshari, K. R., et al. (2008). Evaluation of lactate and alanine as metabolic biomarkers of prostate cancer using 1H HR-MAS spectroscopy of biopsy tissues. *Magnetic Resonance in Medicine, 60*(3), 510–516.

Tugnoli, V., Mucci, A., Schenetti, L., et al. (2004). Molecular characterization of human gatric mucosa by HRMAS magnetic resonance spectroscopy. *International Journal of Molecular Medicine, 14,* 1065–1071.

Tzika, A. A., Cheng, L. L., Goumnerova, L., et al. (2002). Biochemical characterization of pediatric brain tumors by using in vivo and ex vivo magnetic resonance spectroscopy. *Journal of Neurosurgery, 96*(6), 1023–1031.

van Houten, V. M., Leemans, C. R., Kummer, J. A., et al. (2004). Molecular diagnosis of surgical margins and local recurrence in head and neck cancer patients: A prospective study. *Clinical Cancer Research, 10*(11), 3614–3620.

Voorhis, C. R. W. V., & Morgan, B. L. (2007). Understanding power and rules of thumb for determining sample sizes. *Tutorials in Quantitative Methods for Psychology, 3*(2), 43–50.

Wang, Y., Bollard, M. E., Keun, H., et al. (2003). Spectral editing and pattern recognition methods applied to high-resolution magic-angle spinning 1H nuclear magnetic resonance spectroscopy of liver tissues. *Analytical Biochemistry, 323*(1), 26–32.

Wang, Y., Bollard, M. E., Nicholson, J. K., & Holmes, E. (2006). Exploration of the direct metabolic effects of mercury II chloride on the kidney of Sprague-Dawley rats using high-resolution magic angle spinning 1H NMR spectroscopy of intact tissue and pattern recognition. *Journal of Pharmaceutical and Biomedical Analysis, 40*(2), 375–381.

Warburg, O. (1956). On the origin of cancer cells. *Science, 123*(3191), 309–314.

Waridel, F., Estreicher, A., Bron, L., et al. (1997). Field cancerisation and polyclonal p53 mutation in the upper aero-digestive tract. *Oncogene, 14*(2), 163–169.

Wilson, M., Davies, N. P., Grundy, R. G., & Peet, A. C. (2009). A quantitative comparison of metabolite signals as detected by in vivo MRS with ex vivo 1H HR-MAS for childhood brain tumours. *NMR in Biomedicine, 22*(2), 213–219.